

Relaxation Behavior of Néel Temperature in Micro and Nanosized Particles of CaMnO_3

*Kompany.A ,Ghorbani Moghadam.T, Kafash. S, Hosseini. S. M,

Ebrahimizadeh Abrishami. M

Department of Physics, (Materials and Electroceramics Laboratory) Ferdowsi University of Mashhad, Iran

**E-mail: kompany@yahoo.com*

** Corresponding Author. Tel.: +989153131366*

Abstract

Micro and Nanosized powders of CaMnO_3 were prepared by the conventional solid state- reaction and sol-gel procedures, respectively. The X-ray patterns indicated that both types of the powders have orthorhombic symmetry structure at room temperature. Further characterizations of the samples were performed employing SEM and TEM techniques. The oxygen content in the prepared powders were determined by EDS which revealed that the amount of oxygen in the samples synthesized via the sol-gel method is less than that of the samples prepared by the solid-state reaction. The phase transition temperature from antiferromagnetic to paramagnetic was found to be slightly higher in sintered O ring samples made from nanopowders. These results can be due to the double exchange $\text{Mn}^{3+}\text{-O-Mn}^{4+}$ interaction and also electron hopping mechanism which occurs more in the samples made from nanopowders. The frequency dependence of the Neel temperature and the shape of the hysteresis loop, observed in both types of the samples, can be attributed to the reduction of relaxation time with increasing the frequency.

Keywords: *Antiferromagnetic, Néel temperature, Hysteresis loop, Oxygen deficiency, Relaxation*

1. INTRODUCTION

In the past two decades the manganese oxides, because of their interesting electrical, magnetic and thermoelectric properties have been studied extensively. They exhibit large magnetoresistance and unusually charge and magnetic ordering. These effects are believed to arise due to the strong coupling among the charge, lattice, and spin_magnetic_degrees of freedom [1]. CaMnO_3 is a so called parent compound for many manganese oxide systems exhibiting colossal magnetoresistance such as $\text{Ca}_{1-x}\text{La}_x\text{MnO}_3$ and $\text{Ca}_{1-x}\text{Sr}_x\text{MnO}_3$ [2]. The CaMnO_3 , crystallizing in a perovskite type structure with space group Pnma, is a G-type antiferromagnetic (AFM) insulator with additional weak ferromagnetic component in its ground state [3]. When oxygen content decreases, the CaMnO_{3-x} phases show stronger double exchange interactions with ferromagnetic ordering and increasing the T_N

[4]. For example, $\text{CaMnO}_{2.5}$ shows an antiferromagnetic transition to paramagnetic around $T_N \sim 350\text{K}$ [5]. This effects are explained by the incorporation of Mn^{3+} cations when the oxygen are reduced, which induces $\text{Mn}^{3+}-\text{O}-\text{Mn}^{4+}$ ferromagnetic double-exchange interactions and the increase of the conduction by electron hopping mechanism [6]. In addition, increasing of T_c in manganese oxides by particle size reduction is can be due to compaction of the unit cell of the lattice and reduction of the unit cell anisotropy [7]. However, recently, many works have been published related to structure and magnetic properties of CaMnO_3 at high magnetic fields [8-12]. In this paper we have studied magnetic properties of CaMnO_3 samples prepared by both sol-gel and conventional solid state reaction methods at low magnetic fields and investigated the relaxation behavior in these samples.

2. EXPERIMENTAL

Nano and micro powders of CaMnO_3 were prepared by sol-gel and conventional solid state reaction methods from a stoichiometric mixture of $\text{Ca}(\text{CH}_3\text{COO})_2 \cdot \text{XH}_2\text{O}$ and $\text{Mn}(\text{CH}_3\text{COO})_2 \cdot 4\text{H}_2\text{O}$. All the synthesized powders were calcinated at different temperatures. However the lowest temperature at which manganese oxides perovskite structure was established was found to be 800°C . Both samples were pressed into O ring at pressure 100bar and sintered at 900°C . X-ray diffraction (XRD) analysis was carried out using $\text{CuK}\alpha$ radiation. Lattice parameters were obtained from the analysis of the x-ray data. Scanning (SEM) and transmission electron microscopy (TEM) techniques were used to observe the particles morphology as well as nano structures of the sintered samples. The samples prepared as O rings were magnetized, using a coil to produce a magnetic field, and also measured in a magnetic setup, using the Faraday effect with $H < 30 \text{ A/m}$. The Néel temperature and magnetic permeability of both types' samples were measured, as a function of temperature at three different frequencies. The hysteresis loops were measured at 77K by applying an AC current with frequency values 10 KHz and 100KHZ. The shape of the hysteresis loops observed on the oscilloscope depends on the applied current intensity, which is related to the magnetic field of samples (B) [13]. Finally, AC hysteresis curves of both samples are measured and compared.

3. RESULTS AND DISCUSSION

A-Charactization

The XRD patterns of CaMnO_3 powders calcinated at 800°C are given in Fig.1, which indicate that both samples are single phase with an orthorhombic symmetry. Structure refinements of these samples from x-ray data were performed in the orthorhombic space group Pnma with parameter constants presented in Table 1.

The TEM image of the CaMnO_3 nanopowders shown in Fig. 2 indicates that the nanoparticles shape is spherical. The average particles size is about 85 nm.

B-SEM and EDS Analysis

The SEM images of the CaMnO_3 samples sintered at 900°C , prepared from conventional solid state reaction and sol-gel techniques, are shown in Fig.3. The grains size of CaMnO_3 sample made from the nanopowders synthesized via sol-gel method, Fig.3 (a), are about 100–200 nm and are highly homogeneous in comparison with the grains of the sample prepared from micropowders, Fig.3 (b).

The Oxygen content determined by EDS analysis for the CaMnO_3 sample prepared by sol-gel method is less than that of the sample prepared by conventional solid state reaction.

C-Magnetic properties

Plotting the magnetic permeability of CaMnO_3 samples versus temperature helps to determine the Néel temperature and test the homogeneity of the samples. Permeability was obtained by measuring the inductance of the samples in a coil on an impedance bridge at different temperatures [13, 14]. Samples were cooled in liquid nitrogen and warmed up gradually with a constant rate. The variation of relative magnetic permeability versus temperature is shown in Fig.4, which shows that above $T_{\text{Néel}}$, permeability decreases with increasing temperature. This can be due to disturbing the domains magnetic ordering, by increasing thermal energy more than the exchange interaction. So at $T_{\text{Néel}}$, transition from antiferromagnetic to paramagnetic occurs. The values of $T_{\text{Néel}}$ obtained at different frequencies for both types of the sintered samples are given In Table 2. The Néel temperature of the sample made from nanopowders are slightly higher than that of the sample made from micropowders. This result can be due to more double exchange interaction $\text{Mn}^{3+}\text{--O--Mn}^{4+}$ and electron hopping which occur in the first sample. The hysteresis curves of the samples are shown in Fig. 5, which are obtained for two frequencies (10KHZ and 100KHZ). Although, the eddy currents are weak, the widening of the hysteresis loops may be due to the increase of eddy currents in our case, since $\text{Mn}^{3+}\text{--O--Mn}^{4+}$ double exchange and electron hopping mechanism have increased with increasing the frequency, leading to the increase of the electrical conductivity. Another way to understand the frequency dependence of $T_{\text{Néel}}$ and the coercivity is considering the forces that act on the domain walls. The state of the system, given by domain wall configuration, is driven by the applied field (varying at a given dH/dt), to relax at lower energies. Coercive and remanence magnetic field measured in both types of the samples are summarized in Table.3. The increase of the coercivity with increasing the frequency in both samples is remarkable. Widening of hysteresis loop is well known in the conductive magnetic materials and it can be attributed to eddy current losses [15, 16]. However, in such low magnetic fields eddy current is negligible. In this case we can use the other theory that at low frequency, dH/dt is low and the system has more time to relax to lower energies, which results in the lowering H_C . With increasing frequency dH/dt increases and the system has less and less time to relax. This effect can be observed as an increase of the domain wall pinning [17].

4. CONCLUSION

The CaMnO_3 nano and micropowder samples have been synthesized by sol-gel and conventional solid state reaction methods, respectively. The X-ray analysis indicates that both structures have orthorhombic phases. The single phase of CaMnO_3 starts to form at calcination temperature of 800°C in both procedures. The average particles size of the synthesized powders is estimated from TEM image and was found to be about 85nm. $\text{CaMnO}_{3-\delta}$ pressed sintered sample made from nanopowders has slightly higher phase transition temperature to paramagnetic state and also wider hysteresis loop than that of bulk samples. This result is due to the double exchange interaction of $\text{Mn}^{3+}-\text{O}-\text{Mn}^{4+}$ and electron hopping which occurs more in the samples made of nanopowders synthesized via sol-gel technique. It was also found that if the hysteresis loop is obtained in an AC magnetic field, the measured Néel temperature and the shape of the hysteresis loop both depend on the frequency of the measuring magnetic field, which can be interpreted by domain wall pinning.

REFERENCES

- [1] J. A. Souza, J. J. Neumeier, R. K. Bollinger, B. McGuire, C. A. M. dos Santos, and H. Terashita, "Magnetic susceptibility and electrical resistivity of LaMnO_3 , CaMnO_3 , and $\text{La}_{1-x}\text{Sr}_x\text{MnO}_3$ ($0.13 \leq x \leq 0.45$) in the temperature range 300–900 K," *Phys. Rev. B* **76** (2007) 024407(1-6).
- [2] Myron B. Salamon, Marcelo Jaime, "The physics of manganites: Structure and transport," *Rev. Mod. Phys.* **73** (2001) 585-592.
- [3] I. Gil de Muro, M. Insausti, L. Lezama, and T. Rojo, "Morphological and magnetic study of $\text{CaMnO}_{3-\delta}$ oxides obtained from different routes," *J. Solid State Chem.* **178**(2005),928-936.
- [4] Z. Zeng and M. Greenblatt, M. Croft, "Large magnetoresistance in antiferromagnetic $\text{CaMnO}_{3-\delta}$ ", *Phys. Rev. B*, (1999) 8784-8788.
- [5] E. Bakken, J. Boerio-Goates, T. Grande, B. Hovde, T. Norby, L. Rormark, R. Stevens, and S. Stolen, "Entropy of oxidation and redox energetics of $\text{CaMnO}_{3-\delta}$," *Solid State Ionics* **176** (2005)2261-2267.
- [6] J. M. D. Coey, M. Viret, and L. Ranno K.Ounaiela, "Electron localization in mixed valence manganites", *Phys. Rev. Lett.* **21** (1995).
- [7] K. Shantha Shankar, Sohini Kar, G.N. Subbanna, A.K. RaychaudhuriS, . Enhanced ferromagnetic transition temperature in nanocrystalline, lanthanum calcium manganese oxide ($\text{La}_{0.67}\text{Ca}_{0.33}\text{MnO}_3$) *Solid State Communications* 129 (2004) 479–483
- [8] Bošković, J. Dukić, B. Matović, Lj. Živković, M. Vlajić, V. Krstić, "Nanopowders properties and sintering of CaMnO_3 solid solutions," *J. Alloys and Compounds* 463 (2008) 282–287.

- [9] E. S. Boz'in, A. Sartbaeva b, H. Zheng, S.A. Wells, J.F. Mitchell, Th. Proffen, M.F. Thorpe, S.J.L. Billinge, "Structure of CaMnO_3 in the range $10 \text{ K} < T < 550 \text{ K}$ from neutrontime-of-flight total scattering," J. Phys. Chem. Solids **69** (2008) 2146–2150.
- [10] Qingdi Zhou, Brendan J. Kennedy, "Thermal expansion and structure of orthorhombic CaMnO_3 ," J. Phys. Chem. Solids **67** (2006) 1595–1598.
- [11] V. Spasojevic, D. Markovic, V. Kusigerski, B. Antic, S. Boskovic, M. Mitric, M. Vlajic, V. Krstic, B. Matovic, "Magnetic properties of nanosized mixed valent manganites CaMnO_3 and $\text{Ca}_{0.7}\text{La}_{0.3}\text{Mn}_{1-x}\text{Ce}_x\text{O}_3$ ($x = 0; 0.2$)," J. Alloys and Compounds **442** (2007) 197–199.
- [12] M. E. Melo Jorge, A. Correia dos Santos, M.R. Nunes, "Effects of synthesis method on stoichiometry, structure and electrical conductivity of $\text{CaMnO}_{3-\delta}$," Int. J. Inorg. Mater. **3** (2001) 5–921..
- [13] C. Medina, E. Amano and R. Valenzuela "a burst system for the isothermal magnetic hysteresis loop of soft ferimagnetic materiales," Rev. Mex. Fis. **29** no. **4** (1983).
- [14] E. Cedillo, J. Ocampo, V. Rivera and R. Valenzuela, "An apparatus for the measuring of initial magnetic permeability as a function of temperature," J. Phys. E: Sci. Instrum. **13** (1980) 383–386.
- [15] G. Bertotti, "Space-time correlation properties of the magnetization process and eddy current losses: Applications. I. Fine wall spacing," J. Appl. Phys. **55** (1984). 4339 (1-9).
- [16] G. Bertotti, "Eddy-current losses in magnetic conductors with abrupt magnetic transitions," J. Appl. Phys. **54** (1983).
- [17] G. V'ertesya, A. Magni, "Frequency dependence of coercive properties," J. Magn. Magn. Mater. **265** (2003). 7–12.

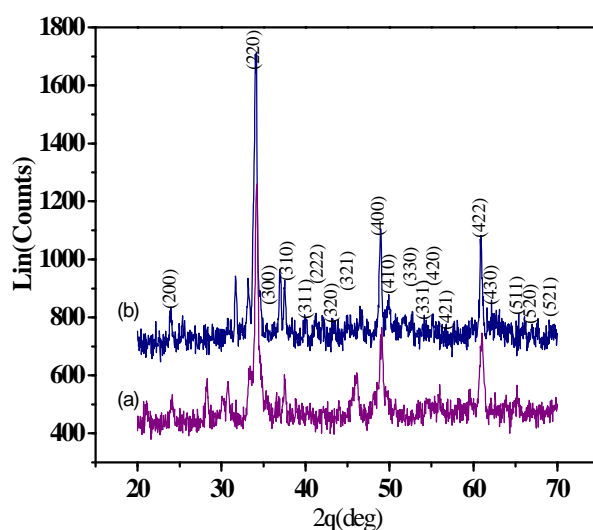


Fig.1 X-ray powder diffraction patterns of CaMnO_3 prepared by

(a) sol-gel and (b)conventional solid state reaction techniques.

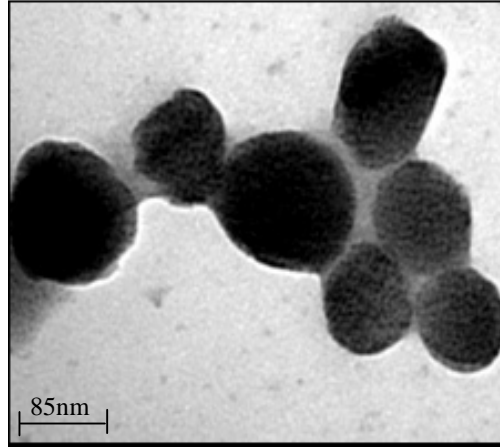


Fig.2 TEM image of the CaMnO_3 nanopowder calcinated at 800°C

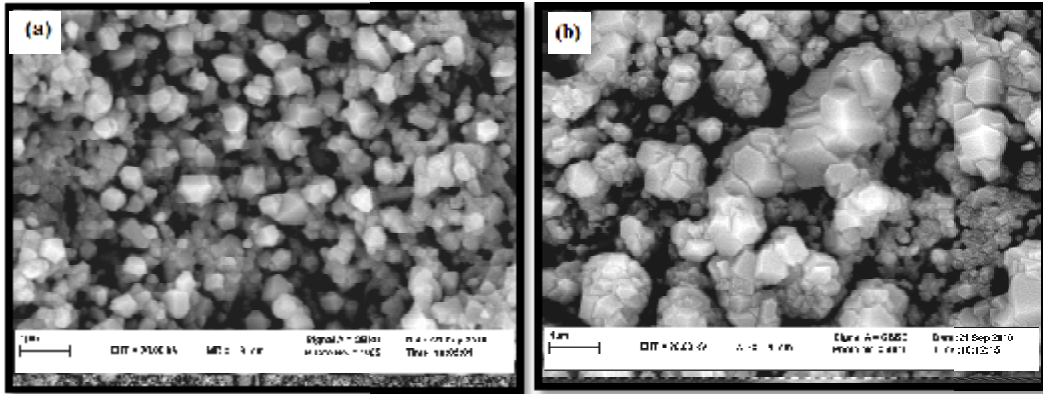


Fig.3 SEM micrograph of the sintered sample, prepared by a) sol-gel and b)conventional solid state reaction methods .

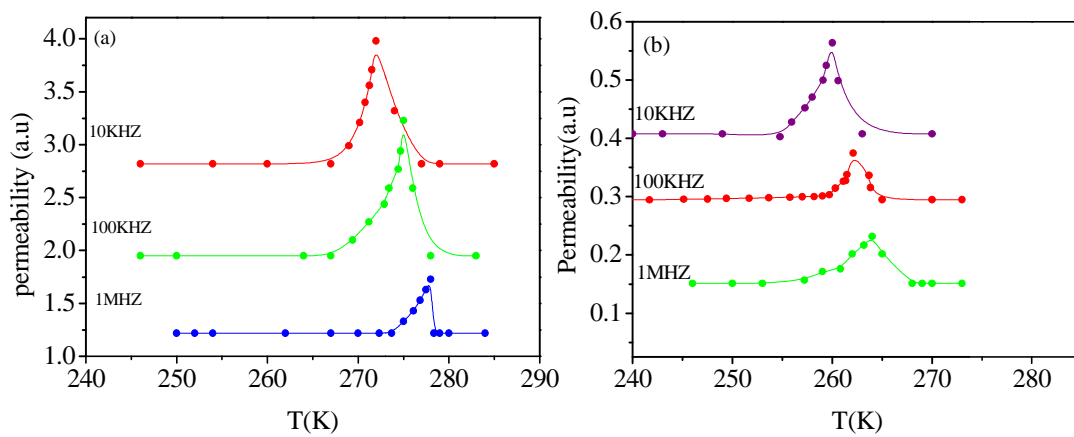


Fig. 4 magnetic permeability of CaMnO_3 prepared by (a) Sol-gel and (b) Conventional solid state reaction methods.

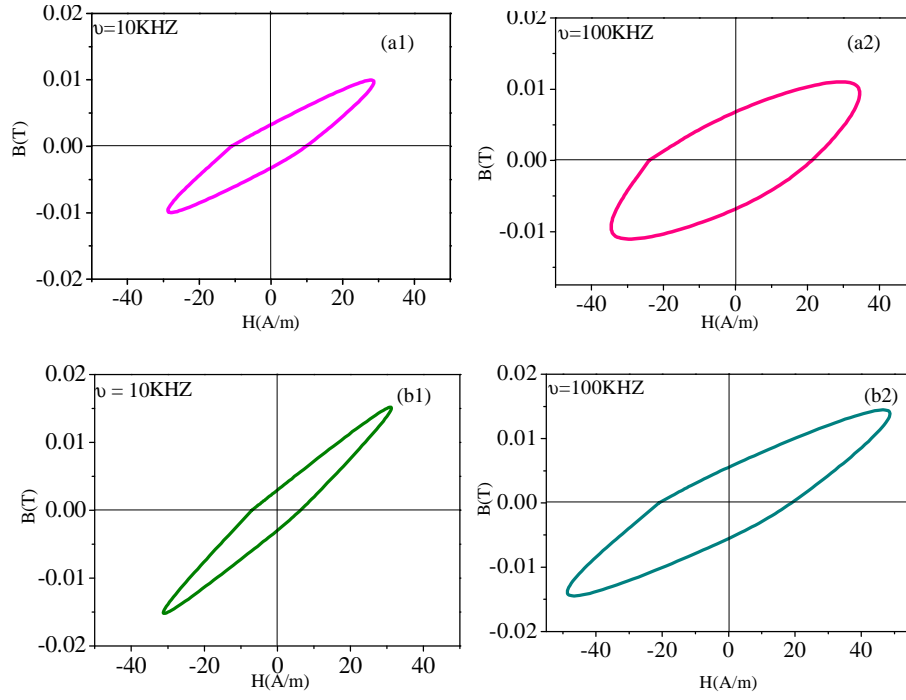


Fig. 5 AC hysteresis curves of CaMnO_3 prepared by (a) nano and (b) micro powders

Table1

Lattice parameter of CaMnO_3 powders

Method	T (°C) (calcination)	2 θ (deg)	d_{hkl}	(hkl)	Phase	Lattice parameter (Å)
Solid state reaction	800	34.17	2.62	(220)	Orthorhombic	a=5.35
		49.07	1.85	(400)		b=7.43
		60.98	1.51	(422)		c=5.28
Sol-gel	800	34.06	2.62	(220)	Orthorhombic	a=5.28
		48.94	1.85	(400)		b=7.45
		60.99	1.52	(422)		c=5.26

Table2

Frequency dependence of Néel temperatures

Sample Prepared of	$\nu = 10\text{KHZ}$	$\nu = 100\text{KHZ}$	$\nu = 1\text{MHZ}$
Nano powders	$T_N = 272\text{K}$	$T_N = 275\text{K}$	$T_N = 277\text{K}$
Bulk powders	$T_N = 259\text{K}$	$T_N = 262\text{K}$	$T_N = 264\text{K}$

Table3

Coercive and Remanence magnetic field of CaMnO_3 samples in $\nu = 10$ and 100KHZ

$\nu(\text{KHZ})$	Sample prepared by Sol-gel		Sample prepared by Solid state reaction	
	$H_c(\text{A/m})$	$B_R(\text{T})$	$H_c(\text{A/m})$	$B_R(\text{T})$
10	10	0.0034	7	0.003
100	25	0.0078	21	0.006